

# Detection of Herpes Biomolecule using Ge-based Dielectrically Modulated TFET

Pooja Raghav, Manisha Bharti and Neha Paras

**Cite as:** Raghav, P., Bharti, M., & Paras, N. (2024). Detection of Herpes Biomolecule using Ge-based Dielectrically Modulated TFET. International Journal of Microsystems and IoT, 2(10), 1246-1253. <https://doi.org/10.5281/zenodo.14167709>



© 2024 The Author(s). Published by Indian Society for VLSI Education, Ranchi, India



Published online: 30 October 2024



Submit your article to this journal:



Article views:



View related articles:



View Crossmark data:



**DOI:** <https://doi.org/10.5281/zenodo.14167709>

Full Terms & Conditions of access and use can be found at <https://ijmit.org/mission.php>



# Detection of Herpes Biomolecule using Ge-based Dielectrically Modulated TFET

Pooja Raghav<sup>1</sup>, Manisha Bharti<sup>1</sup> and Neha Paras<sup>2</sup>

<sup>1</sup>Department of Electronics and Communication Engineering, National Institute of Technology Delhi, Delhi, India

<sup>2</sup>Special Centre for Nanoscience, Jawaharlal Nehru University, Delhi, India.

## ABSTRACT

In this, dielectrically modulated TFET architecture based on Germanium is proposed for label-free detection of herpes virus. Comprehensive numerical device simulations performed on Silvaco 2D TCAD tool are used to study the performance of these biosensor. By altering the gate voltage, the effectiveness of this biosensor is evaluated based on current sensitivity. This paper will primarily focus on examining the biosensor's sensitivity and performance of a tunnel field-effect transistor (TFET) device. A detailed analysis of the device's ON current, OFF current and subthreshold swing has been conducted. For the specific case of  $k=70$ , the full cavity Ge-DMTFET exhibits an impressive sensitivity of  $7.29 \times 10^8$ , accompanied by an outstanding ION/IOFF ratio of  $2.11 \times 10^8$  and a subthreshold swing of 56.366 mV/dec. The suggested TFET has a lower subthreshold slope, a higher ION/IOFF current ratio, and greater sensitivity as a result of its unique design. As a label-free biosensor, presence and absence of charge of different biomolecules are taken into account when evaluating the sensitivity of the device.

## KEYWORDS

Biosensor; Dielectric modulation; Permittivity; Sensitivity; DMTFET

## 1. INTRODUCTION

Everyone faced lot of difficulties during COVID so it is good to detect any disease timely for minimizing the spread of the virus. As Herpes infections can be asymptomatic or present with mild symptoms in some cases. So timely detection is essential for initiating appropriate medical interventions and preventing complications. Biosensors are of different types, some of them are mentioned in literature such as Electro-mechanical, Piezo-electric, Optical [1-4]. However, there are drawbacks to these biosensors, such as more complicated designs, reduced sensitivity, higher costs. Therefore, field effect transistor-based biosensors are now superior to conventional biosensors for the label free detection due to its various advantages like low power dissipation, higher sensitivity, quick response time and less cost. As particles in nature can be charged or neutral so FET based biosensors are good choice for detection of charged particle, it can accommodate charge at the interface and for neutral particle, no need to show any charge. And as they consume less power which makes them suitable for portable biosensing devices, so they are becoming increasingly important among the various types of biosensors. Basically, label-free biomolecule detection takes advantage of various properties of biomolecules like dielectric constants and the charges associated with it[5]. Moreover, FET-based biosensors have large production capabilities, smaller size & lower cost. Herpes is a contagious disease that spreads from person to person and is brought on by the varicella zoster (VZV) virus, which also causes chickenpox. Herpes viruses are a family of DNA viruses, the virus that causes chickenpox remains in a person's body for the remainder of their life.

Furthermore, the virus might reactivate as herpes years later. Another name for herpes is shingles or smallpox. Although herpes is not fatal, it can cause excruciating pain [6]. The main differences between the two forms of Herpes Simplex, or simply plain Herpes, are the infection and symptom changes by HSV-1 and HSV2. Throughout the world, herpes simplex type 1 virus (HSV-1) is an endemic infection that spreads very quickly [7]. Herpes symptoms, such as open sores or blisters at the infection site termed ulcers, can be caused by both HSV-1 and HSV-2. Shingles may appear anywhere on the body, but they typically affect the face and the region surrounding the eyes [8]. According to recent research on biomolecule sensing devices which are FET based, TFETs are becoming more significant as dielectrically modulated biosensors, where drain current properties of device are influenced by dielectric permittivity ( $k$ ) of the biomolecules [9].



**Fig. 1** Principle of dielectric modulation

Biomolecules are introduced into the dielectrically modulated biosensor's cavities. The operation of dielectrically modulated biosensors is illustrated in Fig. 1. Permittivity alone will determine the drain current if the biomolecule is neutral; if the biomolecule is charged, then the drain current will be influenced by the permittivity as well as by charged biomolecule's density. TFET's primary drawback is their low on-current (ION), which isn't a big deal for

applications involving biomolecule sensing. Various methods are being explored to improve ION and subthreshold swing (SS), such as using a gate dielectric with a higher permittivity. A double gate TFET produced two channels when compared to a single gate TFET, producing better device results in form of electrical parameters like, ION, ION/IOFF, SS, and threshold voltage (VTH) [10]. Subthreshold swing, the reciprocal of subthreshold slope, serves as an indicator of device efficiency [11]. A lower subthreshold slope implies better device performance. The graph clearly demonstrates that the full cavity configuration exhibits a reduced subthreshold slope, signifying improved device characteristics. This observation underscores the enhanced performance and efficiency of device when the cavity is filled, providing valuable insights into the optimal operating conditions for the DMTFET. Fig. 5 (e) reveals a noteworthy observation: as drain voltage increases for the partial cavity configuration, bands within the device move closer, indicating improved tunneling. This proximity leads to heightened sensitivity, as more efficient tunneling occurs with increasing drain voltage.

In label-free detection, the probe or device directly detects or senses the test material instead of using a tagged entity to do so. Any foreign molecule that is chemically or momentarily bonded to the target molecule in order to identify its presence or activity is referred to as a label because it has the ability to change the molecule's inherent characteristics. The primary benefit of label-free detection is the ability to obtain more precise information because the techniques employ only biomolecules. Because of a number of inherent drawbacks, labelled biosensing is not appropriate for the actual verification of biomolecular interactions. A less costly option is dielectric modulation and faster label-free biomolecule detection method than labelled biosensing techniques. [12][13]. Molecular biophysical characteristics including molecular weight, permittivity, refractive index and molecular charge are used by label-free detection techniques to track the presence or activity. Therefore, molecules possessing these characteristics are eligible to label-free detection.

## 2. DEVICE STRUCTURE AND SIMULATION SETUP

### 2.1 Device Structure and Specifications

The proposed full cavity Ge based DMTFET is schematically represented in Fig. 2 in that order [14]. In the full cavity Ge-based DMTFET, the metal gate sits atop a fully etched gate dielectric, and a 2 nm insulating layer covers the entire length to reduce gate leakage. Conversely, the partial cavity Ge-based DMTFET features a 2 nm insulating layer across its length for gate leakage control.

This design variations aim to optimize device performance by managing gate leakage through strategic cavity and insulator integration [15]. This representation, which is typically taken into consideration for simulation of this device DMTFET, is the 2D top view of the sensor devices. The dual-gate

arrangement improves electrostatic control by guiding field lines from one gate to the other, avoiding termination in the channel. This configuration enhances precision in regulating the gate within the channel. Because of more band bending in tunnelling, it lowers depletion width and raises electric field surrounding the junction. The source gives the charge carriers so the doping in the source ( $10^{20}$ ) is larger than in the other regions.

Due to the device's two channels for current flow, ON state current is also increased when compared to a single gate TFET. Source and drain of biosensor, as shown in below Fig. 2, are 40 nm apart, making its total length 100 nm. The cavity structure is inserted below the both gate terminals in these structures.

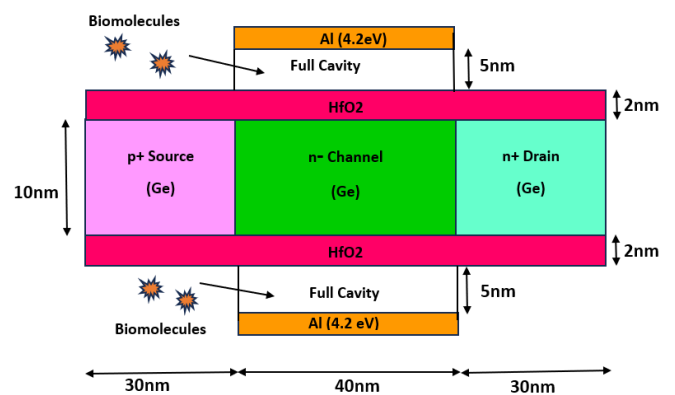


**Fig. 2** Schematic of full cavity Ge based DMTFET

Structure contains two cavities. Each cavity has a 5 nm width. Therefore, for full cavity Ge-based DMTFET, the active area (cavity length  $\times$  cavity width) which senses the biomolecule is approx. 200 nm<sup>2</sup> and 100 nm<sup>2</sup> [16]. A 2 nm (nanometer) insulating layer of hafnium oxide (HfO<sub>2</sub>) is employed to control the gate leakage current. Germanium is used in source, channel, and drain because it has a low bandgap, which increases the tunnelling barrier height and improves the ON state performance of device [17].

**Table. 1** Parameters used for the biosensor

## 2.2. Device Simulation

The Silvaco TCAD is used to carry out the device simulations. All simulations are done at  $V_{DS}=1V$ . The tunnelling probability of carriers through the tunnelling junction is computed, using the well-known idea of non-local (NL) band-to-band tunnelling. The mobility of carriers in the doping-dependent Fermi model is influenced by changes in doping concentration at various locations. To manage the much doped source and drain areas, consideration is given to Fermi Dirac carrier distribution. Carrier recombination is modeled using the Shockley Read Hall (SRH) approach [18].

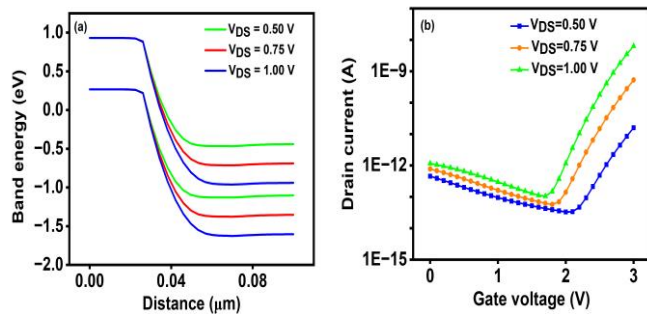


**Fig. 3** (a) energy band diagrams corresponding to different  $V_{DS}$  for full cavity, (b) drain current for full cavity when cavity contains air

In the analysis of Fig. 3 (a), an observation was made that the bands within the device move closer as the drain voltage increases. This proximity results in improved tunneling, enhancing sensitivity. The closer bands facilitate more efficient electron transfer across the device. Correspondingly, Fig. 3 (b) illustrates as the drain voltage increases, there is a clear elevation in the drain current. This phenomenon can be attributed to the heightened tunneling effect, indicating a direct correlation between drain voltage, sensitivity, and increased drain current, showcasing the impact of voltage on the device's performance. These band diagrams and drain currents are calculated when contained air only.

Assume cavity is completely filled during presence of a biomolecule, representing dielectric modulation from  $k=1$  to  $k=70$  within nanogap cavity region [19]. In cavity areas, an appropriate material is taken into account. Additionally, in accordance with earlier reports based on numerical device simulations, this material's dielectric constant ( $k$ ) and surface charge density ( $\rho$ ) has been precisely modified to depict the impact of biomolecule conjugation on carrier transport mechanism and device electrostatics of the biosensor. By assessing alterations in the electrical characteristics of the device, one can identify and measure the concentration of the specific biomolecules under investigation [20]. In the analysis of Fig. 2.2 (a), an observation was made that the bands within the device move closer as the drain voltage increases. This proximity results in improved tunneling, enhancing sensitivity. The closer bands facilitate more efficient electron transfer across the device. Correspondingly, Fig. 2.2 (b) illustrates as the drain voltage increases, there is a clear

Structural Specifications	Full Cavity
Source/ Drain length [14]	30nm
Channel length [14][15]	40nm
Channel thickness [15]	10nm
Gate metal work function on channel	4.2 eV (Aluminum)
Cavity width [16]	5nm
Cavity length [16]	40nm
Oxide thickness of Gate ( $HfO_2$ )[14]	2nm
Source doping (Ge) [14]	$1E20$
Channel doping (Ge) [14]	$1E15$
Drain doping (Ge)[14][15]	$1E18$

elevation in the drain current. This phenomenon can be attributed to the heightened tunneling effect, indicating a direct correlation between drain voltage, sensitivity, and increased drain current, showcasing the impact of voltage on the device's performance. Note that this kind of simulation approach is an oversimplified representation of the actual circumstance [21].

Most experimental research on biosensors that are modulated by dielectric effects primarily concentrates on assessing their electrical properties in dry conditions. The absence of biomolecules is simulated with air environment ( $k=1$ ,  $\rho = 0$ ). During biomolecule conjugation, the cavity is assumed fully occupied, representing dielectric modulation as the cavity's dielectric constant changes from 1 to 70 ( $\rho = 0$ ) [22]. It provides a satisfactory alignment with experimental findings on a qualitative level, offering a dependable means to scrutinize the fundamental physics governing the transduction mechanism. This, in turn, facilitates the exploration of effective strategies for optimizing the design of biosensors with dielectric modulation.

## 3. RESULTS AND DISCUSSION

This sections discusses the simulation results of biosensors considering dielectric constants, charges and temperature effect. Detailed examination of ON current variations in response to variously charged biomolecules and nanogap configurations.

### 3.1 Effect of Neutral Biomolecules on Sensitivity Through Drain Current Analysis

As dielectric permittivity of neutral or uncharged biomolecules increases, more charge carriers—that is, electrons can tunnel through the tunnelling width of barrier at source or channel intersection [23]. The gate's ability gets better to control the channel when the permittivity of biomolecules rises.

Consequently, a larger electric field is produced at the tunnel junctions where the tunneling barrier's width is decreased. When the dielectric constant in cavity is less then significant potential drop is seen across the cavity and when dielectric constant is more then comparatively lesser potential drop is observed so we can say surface potential got increased after biomolecule conjugation.

The study explores influence of various biomolecules on a device performance, using a sensitivity scale denoted by the parameter "k." An environment containing only air is considered as a baseline with a sensitivity of  $k=1$ , indicating absence of biomolecules [24].

Fig. 4 (a) presents the Energy Band Diagram, highlighting enhanced tunneling in the presence of the herpes virus. The graph depicts alterations in energy levels, illustrating improved tunneling characteristics when exposed to the herpes virus. The changes in the energy band diagram provide visual evidence of the virus's influence on the device's electrical properties, showcasing the potential impact on tunneling efficiency in the presence of herpes [25].

In Fig. 4 (b), the graph compares drain currents for devices in the presence and absence of herpes. It reveals significantly higher current levels when herpes is present in the cavity. Notably, the difference between currents with a filled and empty cavity is substantial [26]. This pronounced contrast in current levels indicates a heightened sensitivity presence of herpes. Larger disparity underscores device's heightened responsiveness to the introduction of herpes, suggesting a notable impact on the electrical characteristics of the system.

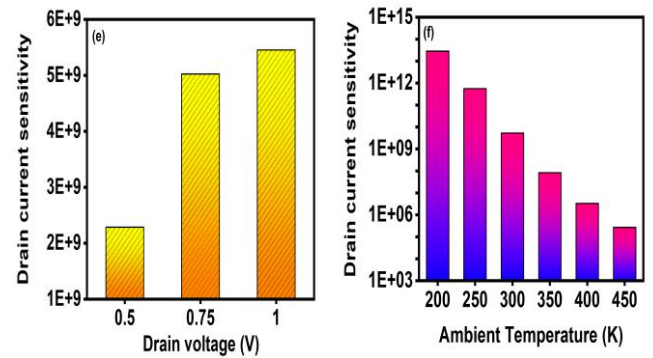
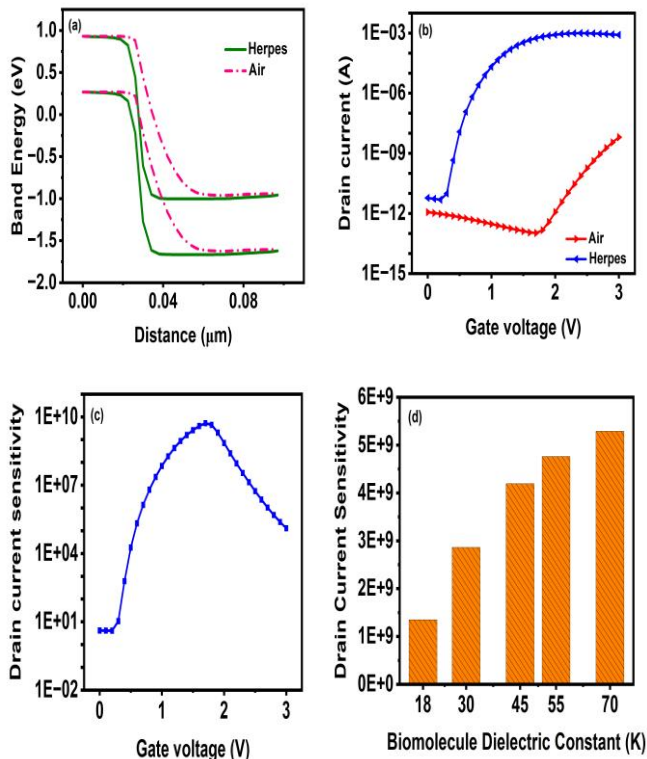


**Fig. 4** (a) energy band diagram showing better tunnelling in presence of herpes (b) comparison of drain currents with herpes and without herpes (c) drain current sensitivity (d) sensitivity corresponding to different diseases (e) sensitivity at different drain voltages (f) sensitivity at different temperatures

Fig. 4 (c) shows sensitivity for gate voltage of 0 to 3V when cavity contains herpes and air. Sensitivity is calculated from the equation given in (1). Drain current sensitivity ( $S_{current}$ ) of DMTFETs is used to estimate their sensing performances. It is formulated as shown in equation (1) ;

$$S_{current} = \frac{I_D^{bio} - I_D^{air}}{I_D^{air}} \quad (1)$$

where,  $I_{D\ air}$  and  $I_{D\ bio}$  are drain current, before ( $k=1$ ) and after ( $k > 1$ ) in biomolecule gate and drain bias depended on the sensitivity profiles are taken into account to determine appropriate biasing condition for the procedure of full cavity Ge-based and partial cavity Ge-based DMTFETs [27].

It is important to emphasize that a higher gate bias result in a greater electrostatic potential drop in cavity region, which turn generates an enhanced alteration in the electrostatics of the tunneling junction is achieved through the conjugation with biomolecules. Concurrently, as previously mentioned, the growing gate bias strengthens channel inversion, limiting impact of biomolecule conjugation on tunnelling junction electrostatics. Such conflicting gate bias objectives result in an ideal state of electrostatics. Such conflicting gate bias objectives result in an ideal state of Simultaneously, as indicated earlier, increasing gate bias reinforces channel inversion, reducing effect of biomolecule conjugation on the electrostatics of tunnelling junctions. Such conflicting gate bias agendas result in an optimal sensitivity in the DMTFET operating environment dominated by BTBT [28].

Moreover, fluctuations in the surrounding temperature can affect the sub-threshold current sensitivity in the DMTFET operating regime dominated by BTBT. The lowest avg subthreshold swing (SS) before to conjugation and its subsequent decrease are shown by the partial cavity Ge-based DMTFET. Temperature related increases in DMTFET off state current result in sensitivity reduction. Lastly, a thorough performance comparison between partial and full cavity DMTFETs has been conducted for various biomolecule

parameters [29]. Detecting and quantifying target biomolecules is achievable by assessing difference electrical characteristics of a device [30]. Biosensors, designed for measuring concentrations or the presence of biological analytes is same as the biomolecules and their structures, or microorganisms, consist of three key components: a detector generating a signal, signal transducer, and reading device. These devices find applications not only in research but also in industries such as the food business [31].

The research delves into impact of specific biomolecules, each assigned a distinct sensitivity value ( $k$ ), on the device. Spinal issues for instance, is characterized by a relative permittivity with  $k=18$ , lung illness with  $k=30$ , skin conditions with  $k=45$ , herpes virus with  $k=70$ , and tobacco mosaic virus with  $k=55$ . The findings of this investigation are visually represented in Fig. 4 (d), which illustrates the sensitivity of both devices concerning each biomolecule. It appears that the sensitivity levels vary across different biomolecules, with the herpes virus displaying a sensitivity akin to a  $k$  value of 70. This comparison provides insights into how the device responds to the presence of these biomolecules, offering valuable information for further analysis and applications in relevant fields. In Fig. 4 (e), the plot reveals the determination of the optimal drain voltage for maximum sensitivity in both devices. The correlation between sensitivity and drain voltage is evident, with increased drain voltage positively influencing drain current sensitivity. Moving to Fig. 4 (f), the impact of ambient temperature on maximum drain current sensitivity of DMTFETs is assessed. The graph illustrates a decrease in sensitivity with rising temperature, suggesting that operational modifications are necessary for enhanced sensitivity at higher temperatures [32]. These findings emphasize the significance of optimizing drain voltage and addressing temperature effects for the effective performance of DMTFETs in varying environmental conditions.

### 3.2 Impact of Charged Biomolecules

Herpes is considered a neutral biomolecule based on the results obtained. However, due to the uncertainty about the exact charge of herpes, the research explores the effects of different charge concentrations. Surface charge densities are specifically examined at  $\rho = 1 \times 10^{12} \text{ cm}^{-2}$ ,  $\rho = 0$ , and  $\rho = -1 \times 10^{12} \text{ cm}^{-2}$  to illustrate the impact of varying charge concentrations of herpes. These scenarios are then compared with the effects observed when the cavity contains only air, and results are depicted in Fig. 5 (a). Analysis focuses on relationship between charge concentration and its influence on current. When the cavity contains air alone, this serves as a reference point. The study observes that positively charged biomolecules, including herpes, enhance the presence of electrons in channel. Immobilization of positively charged biomolecules ( $\rho = +ve$ ) in nano cavity results in a decrease in barrier width. This phenomenon is explained by the fact that as density of positively charge biomolecules increases, barrier width decreases, impacting band bending. Conversely, an increase in negative charges and holes in the channel leads to

an expansion of barrier width and a decrease in band bending.

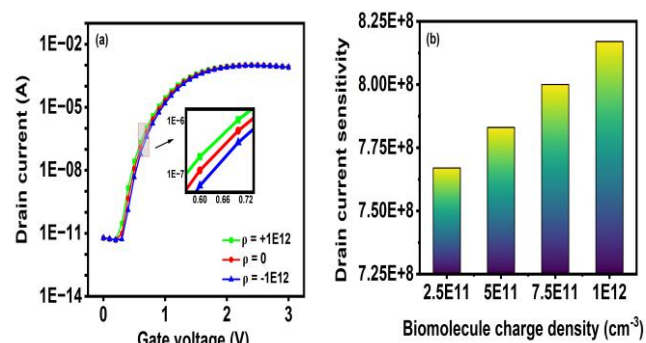


**Fig. 5** (a) drain current considering herpes molecule is negatively charged, neutral and positively charged in full cavity Ge based DMTFET (b) sensitivity for various charge densities for proposed full cavity Ge based DMTFET

Fig. 5 (b) shows drain current sensitivity considering different charges from  $2.5 \times 10^{11}$  to  $1 \times 10^{12}$  on herpes molecule as herpes charge is unknown yet. And as concentration of positive charges enhance electron presence so sensitivity is also increasing with concentration of charges. When a biomolecule enters the cavity, it induces an increase in capacitance at the tunneling junction. This heightened capacitance contributes to an elevation in the device's drain current, consequently augmenting its sensitivity as a biosensor. It is important to note that the sensitivity is not only affected by the mere presence of the biomolecule but also by its specific location within the device and the quantity present. These factors, as highlighted by reference [33], underscore the intricate relationship between biomolecular interactions, capacitance changes, and the resulting impact on the overall sensitivity of the biosensor, providing essential considerations for the design and optimization of such devices. Sensitivity serves as a crucial parameter in discerning variations in target biomolecules, with higher sensitivity indicating a greater likelihood of detecting the target biomolecule. Performance of a biosensor depends on sensitivity value of device. Higher values of sensitivity of device depicts the better sensing capabilities of the biosensor. The detection of biomolecule is more accurate as the sensitivity value increases. During the ON-state, there is a noticeable band alignment at the junction, facilitating the tunneling of charge carriers. This phenomenon occurs when charged neutral biomolecules become immobilized in cavity [34]. Near source or channel junction in tunneling, barrier width diminishes with increasing dielectric permittivity of neutral or uncharged biomolecules. This allows more electrons to tunnel through. Additionally, the inclusion of Ge, which is a low bandgap material located close to the source, plays a role in decreasing barrier width of energy bands in Ge-DMTFET. When a sufficiently high voltage is applied to the gate in the channel, band bending at the source increases, causing alignment. This alignment leads to the initiation of tunneling, resulting in an increased-ON current. [35]. The concentration of charge biomolecules in cavity plays a pivotal role in shaping energy profile of the

system, particularly affecting tunneling barrier width between source or channel and drain or channel junctions. Dielectric permittivity of biomolecules increases, gate's capacity to regulate the channel also intensifies. Notably, the barrier width diminishes when more positively charged biomolecules ( $\rho=+ve$ ,  $k=70$ ) are immobilized in cavity. This reduction occurs because these positively charged biomolecules attract electrons to the channel region, facilitating tunneling. The interplay between charge concentration, dielectric properties, and barrier width showcases the intricate dynamics influencing the device's energy profile, providing critical insights for optimizing its performance in response to varying biomolecule concentrations [36].

### 3.3 Benchmarking of the Proposed full cavity Ge-DMTFET Against Reported Works

This section compares the sensitivity of a full cavity Ge-based biosensor with other reported works on dielectric modulated FET-based biosensors. Sensitivities are derived from published data, hence labeled as 'approximate'. The proposed Ge-based biosensor demonstrates superior sensitivity due to the use of Germanium. However, differences in structural, doping, and dielectric constant specifications among the compared works are noted.

**Table 2** Comparison of Sensitivity with Reported Works

S.No	{Biosensors, K}	Reported Works	Proposed Work
1	DM-DMDG-HS TFET [33], 7	$8 \times 10^3$	$1.30 \times 10^7$
2	DG-PNP Biosensor [25], 3	$1.28 \times 10^5$	$1.89 \times 10^5$
3	DT-DMTFET [14], 2.1	3590	9560
4	FE-CP-TFET based biosensor [36], 8	$2.04 \times 10^7$	$2.08 \times 10^7$
5	HJ TFET [5], 12	$2 \times 10^6$	$1.01 \times 10^8$
6	Buried Strained $Si_{1-x}Ge_x$ DGTFET [38], 10	$2.6 \times 10^5$	$4.23 \times 10^7$
7	DM-DMG TFET [39], 32	$10^6$	$4.15 \times 10^8$

## 4. CONCLUSION

In realm of biosensing technology, proposed Ge-DMTFET biosensors has demonstrated remarkable proficiency by successfully detecting the Herpes virus in a label-free manner. This technology holds significant promise for biomolecule detection, showcasing exceptional sensitivity, particularly when operating in the full cavity mode. For the specific case of  $k=70$ , the full cavity Ge-DMTFET exhibits an impressive sensitivity of  $7.29 \times 10^8$ , accompanied by an outstanding

ION/IOFF ratio of  $2.11 \times 10^8$  and a subthreshold swing of 56.366 mV/dec. One notable advantage of this biosensor is its lower power consumption, operating efficiently at 3V, setting it apart from recently reported biosensors. This characteristic, coupled with its heightened sensitivity, positions the Ge-DMTFET as a promising candidate for advanced biosensing applications. However, before widespread implementation in real-world scenarios, the device might benefit from additional rounds of experimental validation and optimization to fine-tune its performance characteristics and ensure reliability in diverse conditions. The Ge-DMTFET biosensor emerges as a potent tool in the landscape of biosensing, offering the potential for sensitive and specific detection of biomolecules, with the successful demonstration of label-free Herpes virus detection being a noteworthy accomplishment. As advancements continue, further refinement through experimental validation and optimization will pave the way for its integration into practical applications, addressing the evolving needs of real-world biosensing challenges.

## REFERENCES

- [1] Nabaei, R.Chandrawati, and H.Heidari, "Magnetic biosensors: Modelling and simulation," *Biosensors and Bioelectronics*, vol. 103, no. November 2017, pp. 69–86, 2018, doi: [10.1016/j.bios.2017.12.023](https://doi.org/10.1016/j.bios.2017.12.023)
- [2] Y. T. Yang, C. Callegari, X. L. Feng, K. L. Ekinci, and M. L. Roukes, "Zeptogram-scale nanomechanical mass sensing," *Nano Letters*, vol. 6, no. 4, pp. 583–586, 2006, doi: [10.1021/nl052134m](https://doi.org/10.1021/nl052134m)
- [3] S. Busse, V. Scheumann, B. Menges, and S. Mittler, "Sensitivity studies for specific binding reactions using the biotin/streptavidin system by evanescent optical methods," *Biosensors and Bioelectronics*, vol. 17, no. 8, pp. 704–710, 2002, doi: [10.1016/S0956-5663\(02\)00027-1](https://doi.org/10.1016/S0956-5663(02)00027-1)
- [4] F. Yan and H. Tang, "Application of thin- film transistors in label-free DNA biosensors", *Expert Review of Molecular Diagnostics*, vol. 10, no.5, pp -547-549, 2010, doi: [10.1586/erm.10.50](https://doi.org/10.1586/erm.10.50)
- [5] R. Goswami, B. Bhowmick, "Comparative Analyses of Circular Gate TFET and Heterojunction TFET for Dielectric-Modulated LabelFree Biosensing," *IEEE Sensors Journal*, vol. 19, no. 21, pp. 9600- 9609, 1 Nov.1, 2019, doi: [10.1109/JSEN.2019.2928182](https://doi.org/10.1109/JSEN.2019.2928182)
- [6] H. Abdelhamid, I. Khalaf, A. Hussien and R. Abdelbaset, " Dielectrophoretic based Microfluidic for nanoparticles "viruses" separation," *2021 3rd Novel Intelligent and Leading Emerging Sciences Conference (NILES)*, Giza, Egypt, 2021, pp. 1-4, doi: [10.1109/NILES53778.2021.9600490](https://doi.org/10.1109/NILES53778.2021.9600490).
- [7] J. Lee, Y. Jung, S. Shin and T. Yoon, "Analysis of HSV-1 and HSV-2 that cause herpes simplex with Apriori algorithm, decision tree, and support vector machine," *2017 19th International Conference on Advanced Communication Technology (ICACT)*, PyeongChang, Korea (South), 2017, pp. 679- 684, doi: [10.23919/ICACT.2017.7890179](https://doi.org/10.23919/ICACT.2017.7890179).
- [8] Shuyong Zhu & Abel Viejo-Borbolla (2021) Pathogenesis and virulence of herpes simplex virus, *Virulence*, 12:1, 2670-2702, doi: [10.1080/21505594.2021.1982373](https://doi.org/10.1080/21505594.2021.1982373)
- [9] S.Shekhar, J.Madan, and R.Chaujar, "Source/gate material engineered double gate TFET for improved RF and linearity performance: a numerical simulation, *Applied Physics A*, 124(11), pp.1-10, 2018, doi: [10.1007/s00339-018-2158-4](https://doi.org/10.1007/s00339-018-2158-4)
- [10] Rachmawati, Elviwani and A. B. Siregar, "Implementation Combination of Case-Based Reasoning and Rule-Based Reasoning for Diagnosis of Herpes Disease," *2022 6th International Conference on Electrical, Telecommunication and Computer Engineering (ELTICOM)*, Medan, Indonesia, 2022, pp. 210-214, doi: [10.1109/ELTICOM57747.2022.10037979](https://doi.org/10.1109/ELTICOM57747.2022.10037979)
- [11] K. Baruah and S. Baishya, "Performance Assessment of Ge-Source Double-Gate PNP TFET Based Biosensor," *2022 IEEE Region 10 Symposium (TENSYP)*, Mumbai, India, 2022, pp. 1-6, doi: [10.1109/TENSYP54529.2022.9864500](https://doi.org/10.1109/TENSYP54529.2022.9864500).

- [12] Jha, A. Banerjee, S. Dhar, D. Manna and S. Jana Mukhopadhyay, "Review on DMTFET based Biosensor," *2023 International Symposium on Devices, Circuits and Systems (ISDCS)*, Higashiroshima, Japan, 2023, pp. 1-6, doi: [10.1109/ISDCS58735.2023.10153554](https://doi.org/10.1109/ISDCS58735.2023.10153554).
- [13] R. Narang, M. Saxena, R. S. Gupta and M. Gupta, "Dielectric Modulated Tunnel Field-Effect Transistor—A Biomolecule Sensor," in *IEEE Electron Device Letters*, vol. 33, no. 2, pp. 266-268, Feb. 2012, doi: [10.1109/LED.2011.2174024](https://doi.org/10.1109/LED.2011.2174024).
- [14] S. J. Mukhopadhyay, B. Majumdar, K. N. Chappanda, S. C. Mukhopadhyay and S. Kanungo, "Performance Analysis of the Diagonal Tunneling-Based Dielectrically Modulated Tunnel FET for Bio-Sensing Applications," in *IEEE Sensors Journal*, vol. 21, no. 19, pp. 21643-21652, 1 Oct. 1, 2021, doi: [10.1109/JSEN.2021.3103998](https://doi.org/10.1109/JSEN.2021.3103998).
- [15] X. Lin, Z. Gong, Y. Ding, Y. Chen, P. A. Valdes Sosa and M. Joseph Valdes Sosa, "Feasibility Study of Detection of Coronavirus Disease 2019 with Microwave Medical Imaging," *2021 15th European Conference on Antennas and Propagation (EuCAP)*, Dusseldorf, Germany, 2021, pp. 1-4, doi: [10.23919/EuCAP51087.2021.9411374](https://doi.org/10.23919/EuCAP51087.2021.9411374).
- [16] P. D. Tam, M. A. Tuan, T. Aarnink and N. D. Chien, "Directly immobilized DNA sensor for label-free detection of Herpes virus," *2008 International Conference on Information Technology and Applications in Biomedicine*, Shenzhen, China, 2008, pp. 214-218, doi: [10.1109/ITAB.2008.4570538](https://doi.org/10.1109/ITAB.2008.4570538).
- [17] P. Raut, U. Nanda and D. K. Panda, "Design and Modeling of a Label-free JLTFTFET Based Biosensor for Enhanced Sensitivity," *2023 IEEE Devices for Integrated Circuit (DevIC)*, Kalyani, India, 2023, pp. 77-81, doi: [10.1109/DevIC57758.2023.10134791](https://doi.org/10.1109/DevIC57758.2023.10134791).
- [18] G. S. Mishra, N. Mohankumar, S. K. Singh, M. Vamsi and D. S. Reddy, "CV Analysis and Linearity Performance of InGaN Notch Dielectric Modulated Dual Channel GaN MOSHEMT for Reliable Label-free Biosensing," *2022 IEEE International Conference of Electron Devices Society Kolkata Chapter (EDKCON)*, Kolkata, India, 2022, pp. 235-240, doi: [10.1109/EDKCON56221.2022.10032882](https://doi.org/10.1109/EDKCON56221.2022.10032882).
- [19] J. Talukdar, M. Malvika, B. Das and K. Mummaneni, "Sensitivity analysis of Non-uniform TFET with dual material source-based biosensor," *2022 IEEE International Symposium on Smart Electronic Systems (iSES)*, Warangal, India, 2022, pp. 597-600, doi: [10.1109/iSES54909.2022.00131](https://doi.org/10.1109/iSES54909.2022.00131).
- [20] K. C. Singh, P. K. Khuntia, P. Mohanty, S. M. Biswal, B. Baral and S. K. Swain, "Comparative Study of InAs Based Tunnel FET (TFET) Biosensor," *2022 1st International Conference on Circuits, Power and Intelligent Systems (CCPIS)*, Bhubaneswar, India, 2023, pp. 01-04, doi: [10.1109/CCPIS59145.2023.10291959](https://doi.org/10.1109/CCPIS59145.2023.10291959).
- [21] N. N. Reddy and D. K. Panda, "Dielectric Modulated Double Gate Hetero Dielectric TFET (DM-DGH-TFET) Biosensors: Gate Misalignment Analysis on Sensitivity," *2022 2nd International Conference on Artificial Intelligence and Signal Processing (AISP)*, Vijayawada, India, 2022, pp. 1-8, doi: [10.1109/AISP53593.2022.9760561](https://doi.org/10.1109/AISP53593.2022.9760561).
- [22] N. Shaw and B. Mukhopadhyay, "Modeling and Performance Analysis of a Split-Gate T-Shape Channel DM DPDG-TFET Label-Free Biosensor," in *IEEE Sensors Journal*, vol. 23, no. 2, pp. 1206-1213, 15 Jan. 15, 2023, doi: [10.1109/JSEN.2022.3224036](https://doi.org/10.1109/JSEN.2022.3224036).
- [23] N. N. Reddy, V. S. P. Reddy, P. B. S. Jyothi, T. P. Kumar, T. H. Krishna and T. U. Kiran, "Sensitivity Analysis of Dielectrically Modulated Hetero junction InSb/Si SOI-TFET based Biosensor for Cancer Detection," *2023 3rd International conference on Artificial Intelligence and Signal Processing (AISP)*, VIJAYAWADA, India, 2023, pp. 1-5, doi: [10.1109/AISP57993.2023.10134916](https://doi.org/10.1109/AISP57993.2023.10134916).
- [24] S. Gupta, Anju and G. P. Mishra, "Design and Performance Analysis of Z-Shaped Charge Plasma TFET-based label-free Biosensor," *2021 Devices for Integrated Circuit (DevIC)*, Kalyani, India, 2021, pp. 466-449, doi: [10.1109/DevIC50843.2021.9455818](https://doi.org/10.1109/DevIC50843.2021.9455818).
- [25] K. Baruah and S. Baishya, "Performance Evaluation of Double Gate PNP TFET and Extended-Source Double Gate PNP TFET as Label-Free Biosensor," *2022 International Conference on Electrical, Computer, Communications and Mechatronics dcecdsxEngineering (ICECCME)*, Maldives, Maldives, 2022, pp. 1-6, doi: [10.1109/ICECCME55909.2022.9988358](https://doi.org/10.1109/ICECCME55909.2022.9988358).
- [26] D. Wangkheirakpam, B. Bhowmick and P. D. Pukhrabam, "N+ Pocket Doped Vertical TFET Based Dielectric-Modulated Biosensor Considering Non-Ideal Hybridization Issue: A Simulation Study," in *IEEE Transactions on Nanotechnology*, vol. 19, pp. 156-162, 2020, doi: [10.1109/TNANO.2020.2969206](https://doi.org/10.1109/TNANO.2020.2969206).
- [27] M. Verma, S. Tirkey, S. Yadav, D. Sharma and D. S. Yadav, "Performance Assessment of A Novel Vertical Dielectrically Modulated TFET-Based Biosensor," in *IEEE Transactions on Electron Devices*, vol. 64, no. 9, pp. 3841-3848, Sept. 2017, doi: [10.1109/TED.2017.2732820](https://doi.org/10.1109/TED.2017.2732820).
- [28] N. Macambira, P. G. D. Agopian and J. A. Martino, "Impact of process and device dimensions on Bio-TFET Sensitivity," *2018 IEEE SOI-3D-Subthreshold Microelectronics Technology Unified Conference (S3S)*, Burlingame, CA, USA, 2018, pp. 1-3, doi: [10.1109/S3S.2018.8640152](https://doi.org/10.1109/S3S.2018.8640152).
- [29] R. Saha, Y. Hirpara and S. Hoque, "Sensitivity Analysis on Dielectric Modulated Ge-Source DMDG TFET Based Label-Free Biosensor," in *IEEE Transactions on Nanotechnology*, vol. 20, pp. 552-560, 2021, doi: [10.1109/TNANO.2021.3093927](https://doi.org/10.1109/TNANO.2021.3093927).
- [30] Karthik, K.R.N., Pandey, C.K. A Review of Tunnel Field-Effect Transistors for Improved ON-State Behaviour. *Silicon* **15**, 1–23 (2023), doi: [10.1007/s12633-022-02028-4](https://doi.org/10.1007/s12633-022-02028-4).
- [31] P. Dwivedi and A. Kranti, "Overcoming Biomolecule Location-Dependent Sensitivity Degradation Through Point and Line Tunneling in Dielectric Modulated Biosensors," in *IEEE Sensors Journal*, vol. 18, no. 23, pp. 9604-9611, 1 Dec. 1, 2018, doi: [10.1109/JSEN.2018.2872016](https://doi.org/10.1109/JSEN.2018.2872016).
- [32] P. Jain, C. Rajan and M. Panchoe, "A Novel Trench Cavity-Based CP-TFET for Label-Free Biomolecule Detection," *2023 14th International Conference on Computing Communication and Networking Technologies (ICCCNT)*, Delhi, India, 2023, pp. 1-7, doi: [10.1109/ICCCNT56998.2023.10306733](https://doi.org/10.1109/ICCCNT56998.2023.10306733).
- [33] J. Kumar, R. Chaudhary and R. Saha, "Performance Analysis of Dielectric Modulated Dual Material Double Gate Hetero Stack (DM-DMDG-HS) TFET," *2023 International Conference on Intelligent and Innovative Technologies in Computing, Electrical and Electronics (IITCEE)*, Bengaluru, India, 2023, pp. 296-301, doi: [10.1109/IITCEE57236.2023.10090967](https://doi.org/10.1109/IITCEE57236.2023.10090967).
- [34] N. Shaw and B. Mukhopadhyay, "Design and Performance Analysis of Step Channel Stack Oxide DG-TFET for Dielectrically Modulated Bio-sensing Applications," *2022 IEEE Calcutta Conference (CALCON)*, Kolkata, India, 2022, pp. 89-92, doi: [10.1109/CALCON56258.2022.10059827](https://doi.org/10.1109/CALCON56258.2022.10059827).
- [35] Dewan, S. Chaudhary and M. Yadav, "Evaluating the Performance Parameters of Triple Metal Dual Gate Vertical Tunnel FET Biosensor," *2022 IEEE International Students' Conference on Electrical, Electronics and Computer Science (SCEECS)*, BHOPAL, India, 2022, pp. 1-5, doi: [10.1109/SCEECS4111.2022.9740831](https://doi.org/10.1109/SCEECS4111.2022.9740831).
- [36] S. Singh, S. Singh, M. K. A. Mohammed and G. Wadhwa, "Dual Cavity Dielectric Modulated Ferroelectric Charge Plasma Tunnel FET as Biosensor: For Enhanced Sensitivity," in *IEEE Transactions on NanoBioscience*, vol. 22, no. 1, pp. 182-191, Jan. 2023, doi: [10.1109/TNB.2022.3174266](https://doi.org/10.1109/TNB.2022.3174266).
- [37] A. Anam, S. Anand and S. I. Amin, "Design and Performance Analysis of Tunnel Field Effect Transistor With Buried Strained Si<sub>1-x</sub>Ge<sub>x</sub> Source Structure Based Biosensor for Sensitivity Enhancement," in *IEEE Sensors Journal*, vol. 20, no. 22, pp. 13178-13185, 15 Nov. 15, 2020, doi: [10.1109/JSEN.2020.3004050](https://doi.org/10.1109/JSEN.2020.3004050).
- [38] Reddy, N. Nagesh, and Deepak Kumar Panda. "Simulation study of dielectric modulated dual material gate TFET based biosensor by considering ambipolar conduction." *Silicon* **13**.12 (2021): 4545-4551, doi: [10.1007/s12633-020-00784-9](https://doi.org/10.1007/s12633-020-00784-9)

## AUTHORS



**Pooja Raghav** received the B.Tech. degree in Electronics and Communication Engineering from Dr. A.P.J. Abdul Kalam Technical University, India, in 2018. She is currently pursuing M.Tech degree in Electronics and Communication Engineering with specialization in VLSI from NIT, Delhi, India, in 2024. Her current research interests include biological sensors, high-frequency devices, and transport phenomena.

Corresponding Author E-mail: [22221017@nitdelhi.ac.in](mailto:22221017@nitdelhi.ac.in)



**Manisha Bharti** (Member, IEEE) received the M.Tech and Ph.D. degree in Electronics & Communication Engineering from Punjab Technical University, Jalandhar, Punjab and IKG Punjab Technical University, Jalandhar, Punjab in 2017. She is currently working as an Associate Professor with the Electronics and Communication Engineering Department, NIT Delhi, Delhi, India. Her current research interests include Optical Communication Networks & Opto-electronics, Digital & Broadband Wireless Communication, RoF & FSO Communication, Electronic & Photonic Devices.

E-mail: [manishabharti@nitdelhi.ac.in](mailto:manishabharti@nitdelhi.ac.in)



**Neha Paras** received the M.Tech degree in Microelectronics and VLSI Design from Kurukshetra University, India in 2016 and Ph.D. degree in Low Power VLSI Devices from NIT Kurukshetra in 2020. She is currently working as an Assistant Professor with the Special Centre for Nanoscience, JNU, India. Her current research interests include Low Power VLSI Design, Semiconductor Device Design and Modelling, Ferroelectric Memory Devices

E-mail: [neharao1993@gmail.com](mailto:neharao1993@gmail.com)